

# VLBA Phase Referencing for Astrometric Use

*Edward Fomalont*

*National Radio Astronomy Observatory*

*e-mail:* `efomalon@nrao.edu`

## Abstract

The differences in the type of VLBI observations used by radio astronomers to study the structure and motion of radio sources and that associated with IVS and ICRF-based observations, are discussed. An example of a VLBA phase reference observation to determine the gravitational deflection of the sun demonstrates that relative astrometric precision of 0.02 mas can be obtained. The changing structure of virtually all radio sources is now affecting the accuracy of both types of observations and a method to alleviate this problem is demonstrated by determining the position of the radio core very accurately. A scheme is outlined for which the accurate relative positions from phase referencing might be extended to the entire sky.

## 1. Introduction

The observational technique of phase referencing alternates short scans of a calibrator, a compact radio source, with a target in order to determine the *relative* position between the calibrator and target, and to determine the angular structure of the target [1]. These results are obtained with Fourier-transform techniques of the phase delay, and it is a coherent process, meaning that the target can be extremely faint, but signal-to-noise (SNR) can be built up with observing time. The image fidelity is about 50:1 (this does not include strong sources for which self-calibration techniques give  $> 1000 : 1$  SNR) and the relative positional accuracy is often 0.05 mas or better at 8 GHz with an array like the VLBA.

In contrast, the IVS takes a more global view of astrometry. Since quasars are extremely distant, they define a quasi-inertial reference frame much more accurately than stars. But, in order to determine a catalog of quasar positions, the location and space motion of the radio telescopes must also be obtained; hence, this requires the measurement of the earth orientation and rotation, the dynamics of many solar system objects, and the crustal perturbations of the earth's surface. This requires observations over 24-hours of many radio sources and relatively fast cycling around the sky to determine the variable tropospheric refraction [2]. Another major difference with phase referencing is that the main observable is not the phase, but the change of phase with frequency, or the group delay, since the residual (observed - model) phase delay is often in error by more than one revolution. Hence IVS observations span wide-bandwidths in order to measure accurate group delays. This difference in observing technique has perhaps separated the two communities more than is necessary, even though there are some common problems that each need to address to increase the position accuracies.

After an example of a phase-reference experiment using the VLBA in §2, the problems associated with quasar structure and changes are illustrated in §3. This 'jitter' of the quasar emission is becoming one of the sources of errors in obtaining both accurate relative positions and absolute positions. A phase-reference observing scheme that can bridge the high accuracy in obtaining

relative positions to encompass the whole sky, is outlined in §4. Observations are underway with the VLBA to determine if this approach is a feasible method for increasing the accuracy of the ICRF.

## 2. A Phase Referencing Example

About half of the present VLBA proposals use phase referencing, and some examples of the impressive astrometric and astrophysical results are: the determination of the motion of the galactic center [3]; the determination of the Hubble constant by measuring the relative motion of two megamasers in M33 [4]; the gravitational deflection of radio waves by Jupiter [5]; the complex evolution of x-ray binaries [6]; the space motion and parallax of pulsars [7].

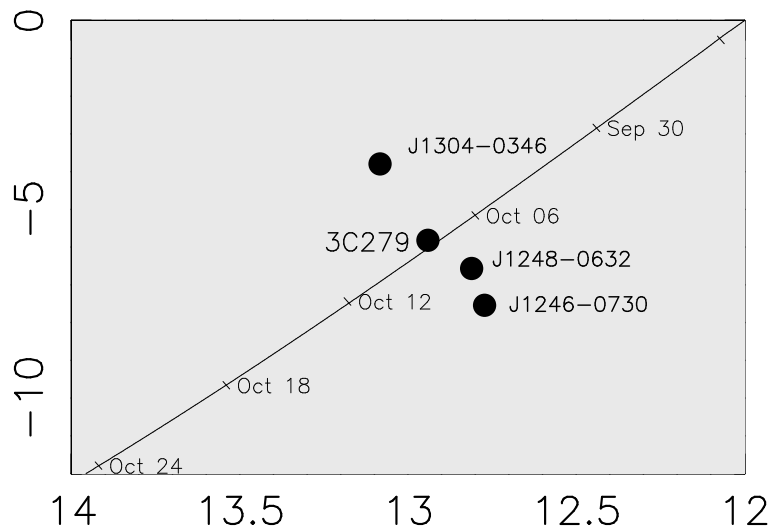


Figure 1. **The Sun-Source Configuration for the October 2005 Solar Bending:** The location of the four radio sources and the motion of the sun during the experiment are shown. Observations were made on October 1, 5, 6, 7, 9, 10, 11 and 18 between UT 17h and 23h. The expected deflection is  $1.75''$  at the solar limb ( $16'$  from the center of the sun) and decreases inversely proportional to the sun-source angular distance. At a sun-source separation of  $2^\circ$ , the deflection is 230 mas and can be measured to an accuracy of less than 1 part in 1000.

We will illustrate VLBA relative astrometry using a classic deflection experiment in October 2005 when the radio source 3C279 passed near and behind the sun [8]. The configuration of 3C279 and three calibrator sources and the sun during October 2005 are shown in Fig. 1. In order to measure the changing relative positions among the sources, the experimental procedure cycled one-min scans among the four radio sources for six hours on each day, and on eight observing days between October 1 and October 18 to measure the relative positions among the sources. The General Relativistic bending parameter  $\gamma$  is 1.0 and predicts a deflection of a radio source at the limb of the sun of  $1.75''$ . Deviations from  $\gamma = 1.0$  are possible with non-Einstein theories and from some large-scale cosmological anisotropies [9]. Because the solar coronal produces a frequency-

dependent deflection of the radio waves (the gravitational deflection is frequency independent), the experiment alternated every twenty minutes among three frequencies, 14, 23 and 43 GHz, in order to remove this frequency-dependent ionospheric component.

The general reduction steps are: First, the most accurate a priori astrometric and geodetic parameters are used during the correlation process for the determination of the model delays using a recent Calc version [10], and updates to the measured earth-orientation and rotation are added off-line. Next, from measurements of the group delay using two 30-min bursts of observations of calibrators over the sky, in an identical manner to IVS observations, a better tropospheric zenith-path delay is determined at the beginning and at the end of the observations for each day [11]. The resultant phase delays among the sources then are sufficiently stable for additional analysis.

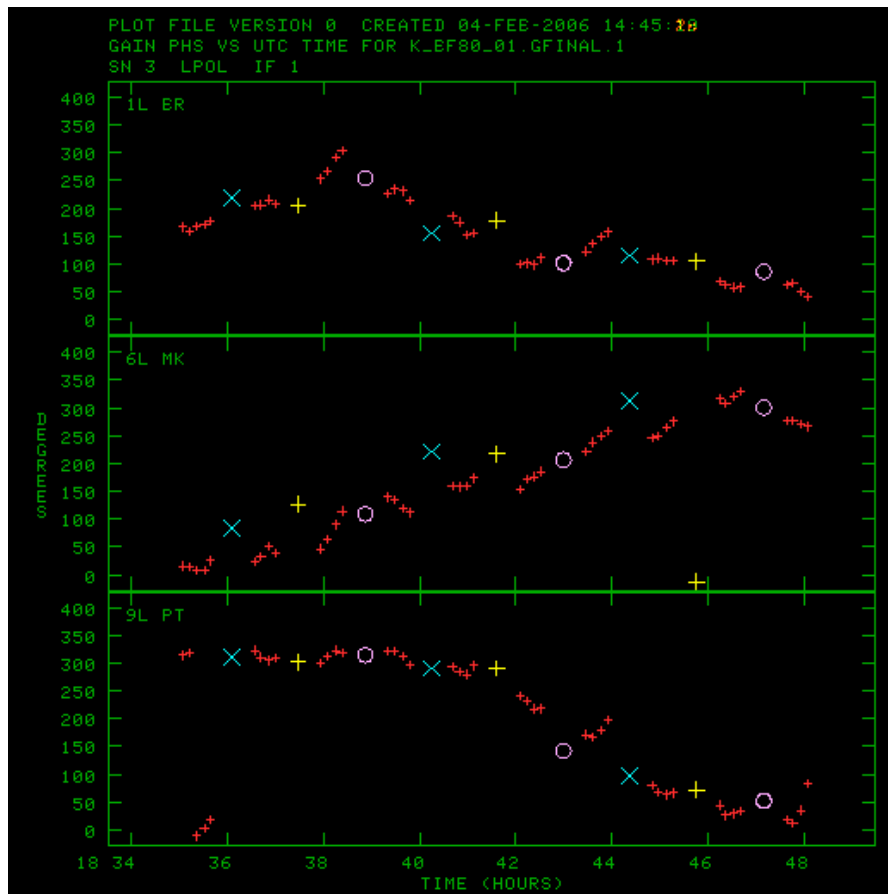


Figure 2. **The Observed Phases of the Four Sources at 23 GHz on October 1:** The three panels show the observed phase versus time over a 13-minute period for the LA-BR (1760 km), LA-MK (4970 km) and LA-PT (236 km) baselines, respectively, after correction for the best-fit residual source positions and the linear phase gradient in the sky. A phase of  $100^\circ$  corresponds to a delay of 12 psec. Each scan was 40-sec in length and the small (red) crosses are for 3C279 every 10-sec during the scan. The other sources, with one average phase per scan are for J1248 cross (white), J1246 circle (blue) and J1304 plus (yellow).

The phases are then analyzed to determine a temporal variable clock correction, plus a constant

position offset for each source on each day, plus a variable phase gradient in the sky in the region of the sources [12, 13]. This phase gradient direction is primary in the elevation direction and is associated with changes in the tropospheric refraction and other remaining astrometric errors. The result of this analysis is shown in Fig. 2 for a 15-min period at 23 GHz on October 1. With the improved relative positions of the sources and removal of the local phase-gradient in the sky, all of the source phases are consistent with the temporal clock term. A rough estimate of the position accuracy can be obtained as follows: The rms phase scatter for a scan is  $15^\circ$  (about 2 psec) for the LA-BR baseline, and this corresponds to a position scatter of about 0.1 mas. This positional accuracy is somewhat independent of baseline-length. When averaged over each scan and over the day, a relative accuracy among the sources is about 0.02 mas.

The reductions are still in progress, but the changes in source position among the three frequencies are consistent with ionospheric refraction, and the ionosphere-corrected positional accuracy is 0.03 mas except when the sources are within  $2^\circ$  of the sun where coronal turbulence decreases the positional accuracy. The preliminary estimated accuracy of  $\gamma$  from this experiment is about  $2 \times 10^{-4}$ , a factor of four better than previous experiments of the gravitational deflection of 3C279.

### 3. The Effect of Source Structure

The effect of source structure has been discussed in previous IVS meetings and it is of concern since the implicit assumption in phase referencing and IVS observations is that the radio sources are stable with time [14]. This variability causes two effects: First, the sources are not point-like and introduce unmodeled changes in the phase and group delays. Since the structure of the radio sources can often be determined using self-calibration techniques of the relevant observations, this correction can be included in the analysis. A more serious and insidious problem is that the *apparent* location of the source may change. In fact, the definition of the source position is arbitrarily defined by the initial detection of the data (fringe-fitting) that defines the location very close to the brightest emission peak. This location is resolution dependent and may not be the stationary point of the radio source (the black hole or the base of the jet) since a variable moving jet component may, in fact, dominate the emission from a central region of the source. This correction requires the knowledge of the evolution of the source and its various components and needs multi-epoch and multi-frequency observations to determine.

An example of the improved position stability obtained with careful modeling of the structure of a radio source is demonstrated by the parallax measurement of G127 [15]. This source is located near the middle of a super-nova remnant (SNR) about 8 kpc away, but it is unclear if it is really associated with the SNR or merely a background extra-galactic radio source, much more distant. Thus, VLBA observations at 8 GHz were made at six-month intervals between May 2002 and April 2004. The phase referencing observations alternated between G127 and an 0.08-Jy calibrator only  $1.5^\circ$  away. Because G127 was much stronger than the calibrator, we used G127 as the primary reference source and measured (via images) the position of the calibrator that was unresolved. Thus, any parallax motion determined for the calibrator would be the reflexive parallax of G127.

The structure of G127 is given in Fig. 3, left contour plot. It is about 6 mas across and aligned nearly east-west. G127 shows the usual structure properties of nearly all compact radio sources, and the radio visibility data has been fit by four Gaussian components using the Caltech Difmap package [16]. It is composed of a point source with about 0.07 Jy, a strong small-scale elliptical component (jet) emanating to the west with about 0.24 Jy, more extended emission with 0.025 Jy

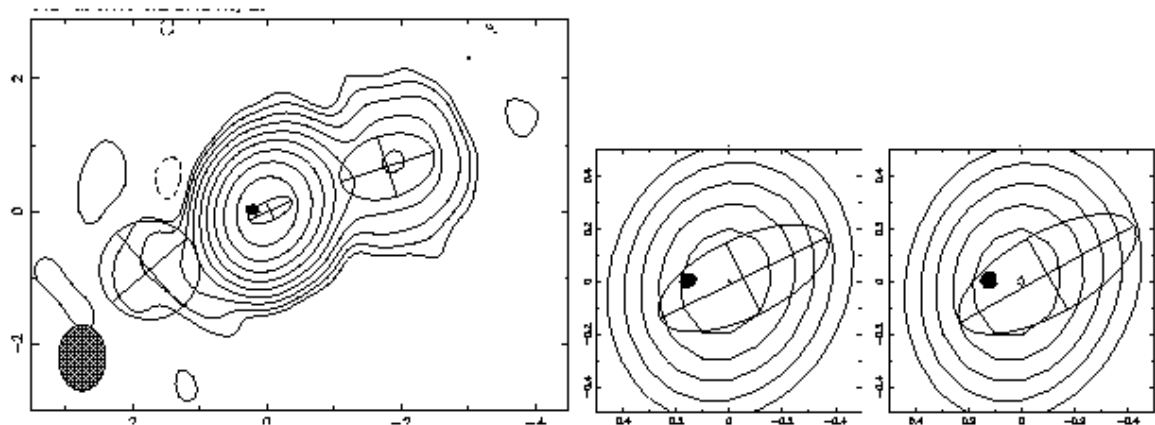


Figure 3. **The Structure Change of G127:** The left-most contour plot shows the structure of G127 for the May 20, 2002 observations. The lowest contour level is 0.2 mJy with levels at multiples of 1,2,4,8,16,32,64,128 and the source extends 6 mas, mostly in the east-west direction. The structure can be fit accurately to the four indicated elliptical components (full-width, half-power levels shown), with the dot as the location of a point component. The two contour plots to the right show the inner-most part of the structure for the May 20, 2002 and Sep 21, 2003 observations, with peak brightness of 0.251 and 0.226 Jy, respectively. The contour levels are at 50,60,70,80,90,98% of the peak. The black dot shows the location of the point component and the ellipse shows the fit to the western jet. The fringe-fit position is at the center of the image, coincident with the brightness peak of this central component. The resolution of all images is  $1.0 \times 0.7$  mas, and the angular scales in mas are labeled.

further to the west, and a faint extended component, east of the point source, with 0.005 Jy. The fitting of the bright central component with a point component and an extended component may appear somewhat arbitrary, but this model is supported by the high resolution studies that show the central emission regions of most quasars contain a point component plus extended emission which generally points in the direction of the more extended emission. The relative location of these two components was obtained naturally from the model fit, and was not assumed during the fit. The location of the point component is generally assumed to be near the compact object in the center of the galaxy or star and is, thus, probably a better approximation to the stationary part of the radio emission than the peak brightness of the central component which is the default source position obtained from the fringe algorithm.

The radio emission and approximate angular size of the central region varied somewhat over the observation period, so that slight structure changes were occurring. A blow-up of the central region of G127 for the May 2002 and September 2003 central regions are shown in Fig. 3, the right two contour plots. Since the positional accuracy of components in relatively simple sources can be obtained to an accuracy of the resolution divided by the signal to noise of the components, which is  $> 100$ , it is, thus, possible to determine their positions to an accuracy 0.01 mas. This modeling shows that the point component is about 0.10 mas east of the brightness peak of the central component, and that its position is 0.04 mas further to the east for the May 2002 observation. The effect of these small changes can be seen in the visibility data of the MK-SC baselines which is 0.08 Jy for the May 2002 data and 0.12 Jy for the Sep 2003 data. This is consistent with the

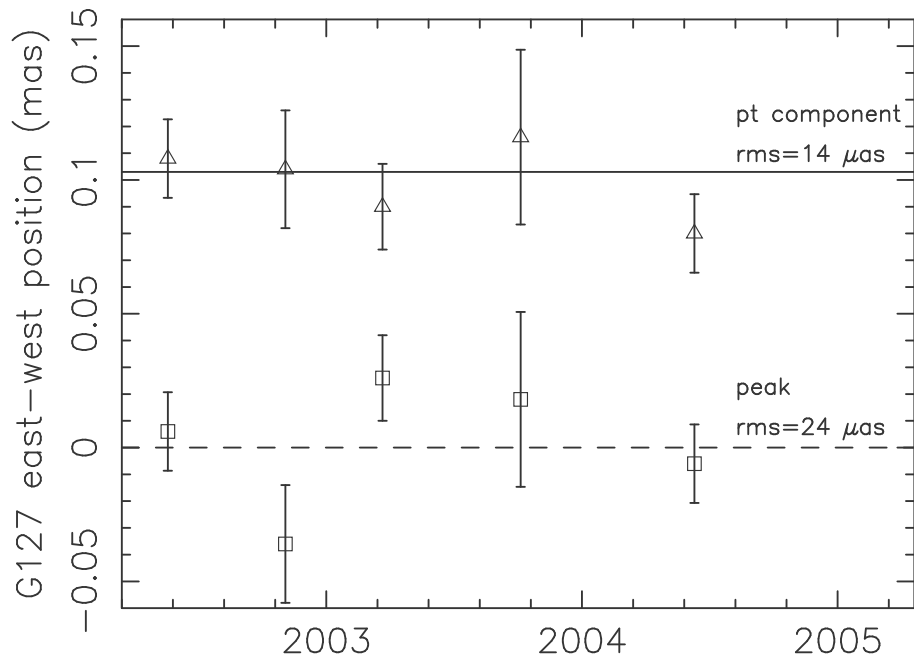


Figure 4. **The Parallax Fit for G127:** The observed east-west relative positions of G127 with respect to the calibrator for the five sessions are shown. The square boxes are the positions with respect to the location of the maximum brightness of the central component in G127, the fringe location. The triangles show the position with respect to the point component determined from the detailed modeling of this bright component. The solid and dashed lines show the best-fit average separation over the five sessions. There is no significant parallax, the rms scatter from the fit decreases when the point component is assumed to be the stationary location of G127.

slightly larger separation of the point component from the nominal center of the source.

Whether the peak of the bright component or the location of the point component is more likely the stationary point in the source can be tested by the quality of the parallax/proper motion fit for the two cases, and these fits are shown in Fig. 4. The top plot shows the fit of the parallax to the location of the point component. Although there is a 0.10 mas offset from the a priori position of G127, the rms fit to the parallax from the mean offset is  $14 \mu\text{as}$  over the five observing sessions. In the bottom plot however, the parallax fit to the peak of the location of the bright component has a significantly larger rms of  $24 \mu\text{Jy}$ . Thus, the point component to the east of the brightness peak has the more stable position when compared with the calibrator source that is nearly unresolved. The formal parallax limit is  $< 0.04 \text{ mas}$  (two-sigma result); hence G127 is more than 25 kpc from the sun and is almost certainly a background galaxy and not associated with the SNR.

The above example demonstrates that for quasars which are about 0.5 Jy (and most ICRF sources are this strong), the location of the point component that is associated with a stable location of the quasar can be determined to an accuracy of about 0.02 mas.

#### 4. The ICRF and Phase Referencing

Can the accurate measurement of the relative position of close sources using phase referencing be extended around the sky to determine more accurate ICRF positions than are now available? Two extensions of phase referencing are needed: First, the area of sky for which sources can be successfully phase-connected must be increased from the maximum radius of  $5^\circ$  now used to at least a radius of  $20^\circ$ . Otherwise, building up a global set of source positions would take the combination of too many small fields. Since there is usually a calibrator within about  $4^\circ$  of any target source, the area for which phase referencing is successful has not been pushed in angular scale. However, the use of several calibrations has been demonstrated to determine the parameters of the variable phase screen over each telescope over large areas to increase the position accuracy and the phase-referencing field of view.

Secondly, the accurate positions obtained in one phase referenced field must be transferred from field to field in order to build up a precise global ICRF. The use of overlapping sources in adjacent fields is the most straight-forward method for this position transfer, but the transferal accuracy and the propagation of zonal errors must be well understood.

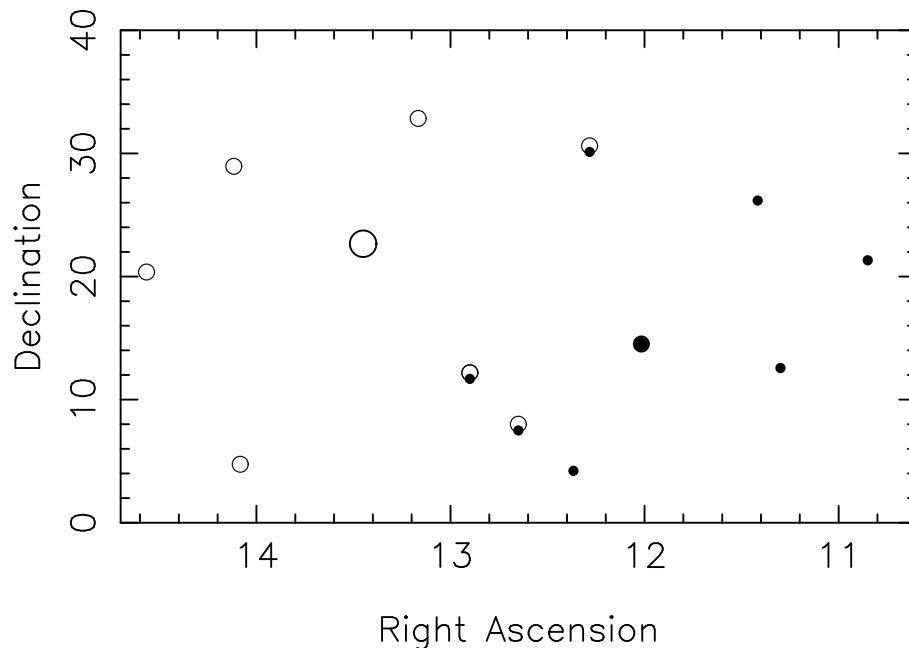


Figure 5. **Source Configuration for Test Observations:** The filled circles show the location of the sources in the phase referencing field 1. The larger circle is that of the primary phase calibrator. The open circles show the sources in the phase referencing field 2, with the larger open circle as the primary phase calibrator. Three sources are in both fields. The location of the field is arbitrary, but was taken near the equator to provide a more challenging test.

Test observations for the VLBA have recently been proposed in order to try to answer the above questions. The observations will consist of phase referencing observations in two adjacent fields, and the proposed configuration of sources is shown in Fig. 5. Each observation will be at S/X band using the identical frequency configuration for IVS observations. Each scan will

be one minute in length and the observations will cycle among eight sources, around a central main phase primary calibrator that will be observed more often. With the use of eight calibrators we hope to determine a phase screen model that is more complicated than a linear drift, and estimate the ultimate size of that multi-source phase referencing. The relatively large number of calibrators is also needed to uncouple the small source position errors (the ICRF accuracy of 0.3 mas is greater than the expected phase-reference position accuracy of  $< 0.05$  mas) from the phase gradient terms. Each field will be observed for three hours. Just before and after the above phase-referencing observations, a 30-min burst of ICRF calibrators over the sky will permit an approximate determination of the global zenith-path delay and other astrometric parameters to lessen somewhat the phase gradients over each field.

We will overlap three sources between the two adjacent fields that will be observed. We know that there must be a registration offset between the two fields because the internal positions will be referenced to different primary calibrators in each field, with an expected position offset of  $\approx 0.2$  mas. However, the offset position of the sources observed in the two fields should be identical. Hence, three overlapping sources seems reasonable. Since one of the overlapping sources is  $20^\circ$  from the other two, some feeling for the size of the zonal errors may be obtained by the difference in the offset among the three sources. This stitching method from small-scale to large-scale areas of sky is similar to the one proposed for Space Interferometry Mission [18].

This data should be easily analyzed in Calc/Solve in the standard manner. The initial AIPS reduction will determine the structure of each source and its contribution to the phase and group delay will be removed [17]. The registration of each structure at the location of the central point component, as in the G127 example, will be attempted. The subsequent reduction in Solve will first use the group delays to determine the approximate solutions and ionospheric refraction, and it is expected that the resultant phase delays will not have any ambiguities. Since the Solve package does not formally fit for a phase-gradient in the sky, it is likely that a few of the astrometric parameters will be solved for in order to simulate a variable phase gradient; eg; troposphere and one nutation term, in addition to the variable clock. Because we are determining the relatively small scale properties of the troposphere and cycling around the  $40^\circ$  region in less than ten minutes, the determination of the troposphere and clock changes over this period of time will be made. This is the main reason why more accurate positions can be obtained compared with the global IVS type observations that determine the approximate all-sky tropospheric properties and clock variations from 30-min to 60-min time scales.

Depending on the accuracy of the above initial observations, further testing and more extended observations of ICRF sources around the sky will be proposed. Extension of this method to higher frequencies, say 23 and 43 GHz, may be difficult because the size of the phase referencing field will decrease too much for effective stitching of positions around the sky [19].

## 5. Acknowledgements

The National Radio Astronomy Observatory is a facility of the National Science Foundation operated under cooperative agreement by Associated Universities, Inc. I thank G. Lanyi and A. Fey for useful discussions about the test observations.



## References

- [1] Beasley, A. J. & Conway, J. E. 1995, ASP Conf. Ser. 82, Very Long Baseline Interferometry and the VLBA, ed. J.A. Zensus, P.J. Diamond & P.J.Napier (San Francisco: ASP), 328
- [2] Ma, C., Arias, E. F., Eubanks, T. M., Fey, A. L., Gontier, A.-M., Jacobs, C. S., Sovers, O. J., Archinall, B. A., Charlot, P. 1998, AJ, 116, 516
- [3] Reid, M. J. & Brunthaler, A, 2005 ASP Conf. Ser. 340, The 10th Anniversary of the VLBA, ed. J. Romney and M. Reid (San Francisco: ASP), 253
- [4] Brunthaler, A., Reid, M. J., Falcke, H., Greenhill, L. J. & Henken, C. 2005, Science, 307, 1440
- [5] Fomalont, E. B. & Kopeikin, S.M. 2003, ApJ, 598, 704
- [6] Fomalont, E. B, Geldzahler, B. J. & Bradshaw, C. W., 2001, ApJ, 558, 283
- [7] Briskin, W.F., Thorsett, S.E., Golden, A. & Goss, W.M. 2003, ApJ 593
- [8] Lebach, D. E., Corey, B. E., Shapiro, I. I., Ratner, M. I., Webber, J. C., Rogers, A. E. E., Davis, J. L. & Herring, T. A. 1995, Phys. Rev. Lett. 75, 1439
- [9] Bertotti, B., Less, L. & Tortora, P., Nature, 2003, 425, 374
- [10] Ryan, J.W., Clark, T.A., Ma, C., Gordon, D., Capretee, D. & Himwich, W.E. 1993, in Contributions of Space Geodesy to Geodynamics: Earth Dynamics, ed D.E. Smith & D. L. Turcotte (Washington:Am.Geophys. Unions), 37
- [11] Mioduszewski, A. 2004, AIPS memo #110, <http://www.aoc.nrao.edu/aips/aipsmemo.html>
- [12] Fomalont, E .B. & Kogan, L. 2005, AIPS memo #111, <http://www.aoc.nrao.edu/aips/aipsmemo.html>
- [13] Fomalont, E. B. 2005 ASP Conf. Ser. 340, The 10th Anniversary of the VLBA, ed. J. Romney and M. Reid (San Francisco: ASP), 340
- [14] Charlot, P. 2002, in IVS 2002 General Meeting Proceedings, edited by R. Vandenberg and K. D. Baver, NASA/CP-2002-210002, 233-242.
- [15] Geldzahler, B. G. & Shaffer, D. B. 1982, ApJ 260, L69
- [16] Shepherd, M. C. 1997 in ASP Conf. Series. 125, Astronomical Data Analysis Software and Systems VI, ed. by G. Hunt & H. E. Payne (San Francisco: ASP), 77
- [17] Greisen, E. W. 1988 in Acquisition, Processing and Archiving of Astronomical Images, ed. G. Longo & G. Sedmak (Napoli: Osservatorio Astronomico di Capodimonte), 125
- [18] Unwin, S. C. 2005 in ASP Conf. Series. 338, 37, ed. P. K. Seidelmann and A. K. B. Monet (San Francisco:ASP), 37
- [19] Jacobs, C. S. et al. 2006 in IVS 2006 General Meeting Proceedings, edited by D. Behrend and K. D. Baver, this volume